Journal of Pharmaceutical Analysis 9 (2019) 437–448

Contents lists available at ScienceDirect

Journal of Pharmaceutical Analysis

journal homepage: www.elsevier.com/locate/jpa

Original Article

Nuclear magnetic resonance based structure of the protoberberine alkaloid coralyne and its self-association by spectroscopy techniques

Kumar Padmapriya, Ritu Barthwal*

Department of Biotechnology, Indian Institute of Technology Roorkee, Roorkee, 247667, India

ARTICLE INFO

Article history:
Received 19 May 2019
Received in revised form
19 August 2019
Accepted 26 September 2019
Available online 26 September 2019

Keywords:
Coralyne alkaloid
NMR spectra
Chemical shift calculations
Restrained molecular dynamics

ABSTRACT

Coralyne is an important alkaloid due to its anti-cancer and other medicinal properties. It targets DNA in cells and acts as human topoisomerase-I poison, telomerase inhibitor and nucleic acid intercalator. It has high tendency to undergo self-association, which is a matter of concern for therapeutic applications. The understanding of its interaction with DNA requires precise knowledge of chemical shifts in Nuclear Magnetic Resonance (NMR) spectra besides self-association. The present study is the first report of a complete assignment of all $^{1}H/^{13}C$ resonances in NMR spectra of coralyne in DMSO-d_6 using one dimensional $^{1}H/^{13}C$ and two dimensional NMR experiments. The chemical shift of all proton and several ^{13}C resonances have also been obtained in D_2O and ethanol-d_6. The same has been calculated using Density Functional Theory (DFT). NMR spectra of coralyne show upfield shift of 0.6–1.2 ppm in aromatic ring protons suggesting stacking interactions. Apart from 11 intra molecular NOE cross peaks in 2D $^{1}H-^{1}H$ ROESY spectra, 3 short distance NOE correlations, H6–10OCH_3, H5–10OCH_3 and H12–16CH_3, give direct independent evidence of the formation of a stacked dimer. The absorbance, fluorescence, circular dichroism and fluorescence lifetime experiments conducted in the present investigations corroborate results obtained by NMR.

1. Introduction

Coralyne is a planar protoberberine alkaloid (Fig. 1), synthesized by treating papaverine with sulphuric acid and acetic anhydride [1–3]. Several antileukemic compounds are known to possess a functional group comprising a well-defined spatial arrangement of one nitrogen and two oxygen atoms, forming a triangle with definite inter atomic distances. It has been suggested that this group contributes in binding to pertinent receptor sites for modification/interruption of biological functions leading to anti-leukemic activity [4]. The oxygen atoms of two neighbouring methoxy groups in coralyne along with nitrogen atom in the ring provide an N–O–O triangle pharmacophore [4] which perhaps renders it anti-leukemic activity with low cytotoxicity against L1210 and P388 leukemia in mice [5]. Coralyne and 5, 6 di-hydro coralyne (DHC) exhibit topoisomerase-I poisoning in cells resistant to camptothecin, a well-known topoisomerase-I poison [6]. Coralyne inhibits telomerase extract from HeLa cells with $IC_{50} = 70\,\mu M$, which is better than that for berberine and piperidino-berberine [7]. It shows improved cytotoxicity upon UV-A treatment through induction of p53 independent apoptosis in MCF-7 breast cancer cells [8]. It has been reported to intercalate in duplex DNA, bind to G-quadruplex and triplex DNA, with higher affinity than berberine [9]. On the other hand, berberine has better selectivity towards triplex DNA than coralyne [9]. Binding of coralyne results in thermal stabilization of poly (C^+:G.C), poly (T:A.T) triplex DNA [10], poly (U:A.U) triplex RNA [11] and t-RNA [12]. It induces duplex formation in single stranded poly (A) by intercalation [13]. It causes greater thermal stabilization in monomeric G-quadruplex DNA than its related alkaloids [7,14]. In an attempt to understand molecular basis of its action using NMR, it is observed that a complete assignment of all protons and carbon atoms in NMR spectra of coralyne does not exist in literature. Till date, only three proton NMR studies have been carried out, which relate to its binding to triplex DNA [15], self-aggregation [16] and interaction with cyclodextrins [17]. In these spectra, only 6 aromatic protons were assigned and considered [16,17].

Coralyne undergoes self-association even in dilute solutions at low ionic strength [10–13] and higher salt concentration promotes aggregation [18]. In 100% ethanol and DMSO, it exists in monomer

Peer review under responsibility of Xi'an Jiaotong University.
* Corresponding author.
E-mail address: ritubfbs@iitr.ac.in (R. Barthwal).

https://doi.org/10.1016/j.jpha.2019.09.006

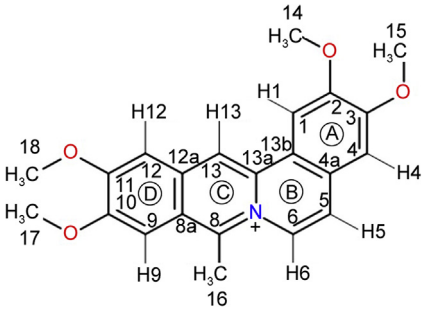

Fig. 1. Chemical structure of coralyne.

form [16]. Effect of solvent on aggregation in ethanol-water mixture has been shown on the basis of observed upfield shifts attributed to stacking interactions using NMR [16]. Mass spectrometry experiments have proved existence of coralyne dimers [16]. The presence of a long lived fluorescence lifetime component with a lifetime of 40.7 ns, due to dimerization, has also been reported [19]. It has been shown that DNA-binding studies of coralyne conducted in 30% ethanolic solution overcome the effect of aggregation of coralyne [20].

Our research group is engaged in exploring interaction of protoberberine alkaloids with DNA by NMR techniques with a specific goal aimed at structure-activity relationship [21]. The knowledge of chemical shift of each and every proton or carbon-13 resonance is absolutely necessary for quantitative assessment of their interaction with duplex/triplex and other forms of DNA, particularly in view of overlap of resonances of coralyne and DNA protons [21]. Further, the understanding of molecular mechanism of their interaction, in monomer or dimer form, with nucleic acids requires knowledge of structural aspects of self-association. We report here a complete assignment of all proton (6 aromatic, 4 methoxy and 1 methyl) and carbon resonances of coralyne using 1D ^{1}H, 1D ^{13}C, 2D $^{1}H-^{1}H$ COSY, $^{1}H-^{1}H$ ROESY, $^{1}H-^{13}C$ Hetero-nuclear Single Quantum Correlation (HSQC) and $^{1}H-^{13}C$ Hetero-nuclear Multiple Bond Correlation (HMBC) experiments in DMSO solvent. We also obtained all proton and several ^{13}C resonances in D_2O and ethanol-d_6. We calculated chemical shift of coralyne in ethanol and gas phase through DFT using wave functions by GAIO method based on B3LYP (Becke, three-parameter, Lee-Yang-Parr) correlation [22–25]. We have carried out 1D proton NMR study of coralyne in aqueous solution, with and without salt, as a function of concentration and temperature. 2D $^{1}H-^{1}H$ ROESY spectra give short distance NOE contacts, which is the first direct and independent proof of dimer formation at molecular level. Structure of self-associated dimer has been obtained by restrained Molecular Dynamics (rMD) simulations. We also performed absorption, fluorescence, Circular Dichroism (CD) and fluorescence lifetime experiments to substantiate self-association.

2. Experimental

2.1. Chemicals

Coralyne chloride hydrate, deuterated water (D_2O) and 3-(Trimethyl Silyl) Propionic-2,2,3,3-d_4 acid sodium salt (TSP) were purchased from Sigma-Aldrich Co. LLC, USA. K_2HPO_4, KCl and EDTA were obtained from Merck KGaA, Darmstadt, Germany. Deionized water required for preparing buffer and coralyne stock solution was obtained from Milli-Q^{TM} water purification system using 0.22 μm filter (Millipore, USA). Coralyne stock solution was prepared freshly in 3 different solvents, water, ethanol and DMSO. Since coralyne is light sensitive, it was kept in dark before taking measurements. Aqueous solution with 120 mM K^+ consisted of 20 mM potassium phosphate buffer containing 10 mM K_2HPO_4, 1 mM EDTA and 100 mM KCl (pH 7.0).

2.2. Absorption spectroscopy

The concentration of coralyne was estimated from absorbance measurements using molar absorption coefficient, $\varepsilon = 14500\ M^{-1}\ cm^{-1}$ and $\varepsilon = 17500\ M^{-1}\ cm^{-1}$ in aqueous and ethanolic solution, respectively at $\lambda_{max} = 420$ nm [13]. The absorbance experiments were carried out using CARY-100 Bio-spectrophotometer (Varian, USA) equipped with Peltier controlled thermostatic cell holder and quartz cell of 1 cm optical path length in the wavelength range of 200 − 600 nm at 25 °C.

2.3. Fluorescence spectroscopy

Fluorescence measurements were performed using Fluorolog-3 Spectrofluorimeter LS55 (make Horiba Jobin Yvon Spex®) equipped with xenon lamp source. The emission spectra were recorded for coralyne samples using excitation wavelength $\lambda_{ex} = 420$ nm in the wavelength range $\lambda_{em} = 435 - 700$ nm in a quartz cell of 1 cm path length at 25 °C.

2.4. Fluorescence lifetime measurements

Fluorescence lifetime measurements were performed using Fluoro-Cube fluorescence lifetime system (Horiba Jobin Yvon) in nanosecond time domain equipped with a Nano LED ($\lambda_{ex} = 405$ nm) source using 1 cm quartz cell at 25 °C. Fluorescence emission was detected at 470 nm by thermoelectrically cooled TBX-04-D detector. All decay traces were measured using 2048 channel analyzer. Typical parameters for these experiments were as follows: time resolution = 0.2 ns, wavelength accuracy = ±0.5 nm, speed = 150 nm/s, TAC range = 200 ns. The analysis of decay curves was based on multi-exponential iterative re-convolution technique using the DAS 6.3 software provided by IBH and the data were fitted for the best chi square value, while errors were obtained as standard deviation from the fit. The fluorescence lifetime measurements for coralyne were carried out in aqueous solution in the presence and absence of salt.

2.5. Circular dichroism (CD) spectroscopy

CD measurements were performed using Chirascan Spectropolarimeter (Applied Photophysics, UK) equipped with Quantum North West TC 125 Peltier unit controlled sample compartment and xenon lamp source. The spectra were recorded at 25 °C in the range of 200 − 600 nm with quartz cell of 0.1 cm path length using scan rate = 100 nm/min, step size = 0.5 nm, time per point = 0.25 s, bandwidth = 1 nm. The final spectrum obtained was average of three experiments. The instrument was continuously purged with pure nitrogen gas using nitrogen generator (make SAS F-DGS, Every, France, model HPNG10/1) throughout the experiment.

2.6. NMR spectra of coralyne

NMR spectra of 500 μL coralyne dissolved in respective solvents were acquired using Bruker Avance 500 MHz Fourier Transform NMR spectrometer at the Central NMR Facility of Indian Institute of Technology Roorkee. Room temperature Triple Resonance Inverse (TXI) probe head was used to acquire NMR spectra. Temperature conditions needed for the experiment were maintained using the

Bruker variable temperature unit. 1D ^{1}H experiments were recorded at different temperatures using the following acquisition parameters: pulse program = zgpr with signal suppression of residual water, data points = 64 Kilo bytes, number of scans = 128, pulse width = 11.49 μs, FID resolution = 0.12 Hz/point, spectral width = 20.0 ppm and length of the recycle delay (D1) = 2.0 s. 2D $^{1}H-^{1}H$ ROESY spectra were acquired in States-TPPI mode using the following acquisition parameters: pulse program = roesyphpr, spin lock duration (p15) = 150 ms, number of scans = 56, data size = 256 (t_1) x 2048 (t_2) complex points, t_{1max} (^{1}H) = 12.7 ms, t_{2max} (^{1}H) = 102.5 ms, spectral width = 20.0 ppm along both F1 and F2 dimension, D1 = 1.5 s. 2D $^{1}H-^{13}C$ HSQC experiment was carried out to obtain proton and carbon correlation using the following acquisition parameters: pulse program = hsqcetgpsi, number of scans = 56, data size = 256 (t_1) x 1024 (t_2) complex points, t_{1max} (^{13}C) = 5.0 ms, t_{2max} (^{1}H) = 64.0 ms, spectral width = 200.0 ppm along F1 dimension and 16.0 ppm along F2 dimension, D1 = 1.5 s. 2D $^{1}H-^{13}C$ HMBC experiment was carried out using the following acquisition parameters: pulse program = hmbcgpndqf with gradient version, number of scans = 56, data size = 256 (t_1) × 2048 (t_2) complex points, t_{1max} (^{13}C) = 63.0 ms, t_{2max} (^{1}H) = 64.0 ms, spectral width = 200.0 ppm along F1 and 16.0 ppm along F2 dimension, D1 = 1.5 s. ^{1}H spectra were calibrated with respect to the resonance of proton of TSP in aqueous solution.

2.7. Theoretical methodology

All theoretical calculations reported in the present study were performed using the Gaussian 98 program package [23]. The geometrical optimization calculations were carried out using the DFT method named hybrid B3LYP employing Cartesian Gaussian-type Orbitals (GTOs), such as STO-3G, 3-21G, 6-31G, 6-31G** and 6-311G** as the basis function for molecular orbital. Hybrid B3LYP is based on Becke's three parameters functional [24] and the correlations provided by Lee-Yang-Parr (LYP) [25]. The proton and carbon chemical shifts of coralyne were calculated from the optimized structure by the GIAO approach installed in Gaussian 98 package. GIAO involves computation of the absolute chemical shielding with respect to electronic environment of individual nuclei. The detailed information on theoretical methodology has already been reported in our previous reports on DFT studies of the protoberberine alkaloids berberine, berberrubine and palmatine [22,23].

2.8. Inter proton distance calculation from 2D $^{1}H-^{1}H$ ROESY data

The NOE distance restraints were calculated from $^{1}H-^{1}H$ ROESY data by ISPA (Isolated Spin Pair Approximation) method using well resolved individual and non-overlapped peaks. The NOE is inversely proportional to sixth power of the distance between two nuclei corresponding to the NOE cross peak. The volume integral of the individual cross peaks corresponding to their respective NOE correlations between two protons i and j (a_{ij}) was calculated using SPARKY 3.114 program [26]. The inter proton distance between two protons i and j (r_{ij}) was then calculated from volume of its NOE cross peak (a_{ij}) using the relation:

$$r_{ij} = r_{ref} (a_{ref} / a_{ij})^{1/6} \quad (1)$$

Where, r_{ref} is the distance between two standard protons, used as reference and a_{ref} is the volume of its corresponding NOE cross-peak. The distance H5 – H6 = 2.44 Å was taken as reference for distance calculations.

2.9. Restrained molecular dynamics (rMD) simulations of coralyne

rMD simulations were carried out using Silicon Graphics Fuel (SGI) workstation with INSIGHT II version 2005 (Accelrys Inc., San Diego) and DISCOVER software program. Geometrically optimized coralyne structure obtained using GAUSSIAN 98 program was used as the starting structure for rMD simulations. Initially, the partial charges on coralyne were fixed to zero using DISCOVER module in INSIGHT II. The molecule was minimized independently using 1000 steps of steepest gradient followed by 1000 steps of conjugate gradient using CVFF force field to remove any strain on the structure before performing simulations. The inter proton distance restraints were fed with upper and lower limit of 0.5 Å. The distance dependent dielectric constant for vacuum, $\varepsilon = 1.0 \times r$, where r stands for distance, was used for calculation of electrostatic interactions. Coralyne dimer molecule was minimized using 2000 steps of steepest gradient followed by 2000 steps of conjugate gradient by keeping force constant of 10.0 kcal/mol. A typical rMD run was carried out for 250 ps at 300 K during which 100 structures were saved.

3. Results

3.1. Chemical shifts from NMR spectra

Ethanol has earlier been used as a co-solvent with water in order to circumvent problem of self-aggregation of coralyne [16,20]. In DMSO solvent, lack of dependence of chemical shift with temperature has been attributed to the absence of self-aggregation [16]. Therefore, we recorded 1D ^{1}H NMR spectra of coralyne at 25 °C in three solvents, namely, ethanol-d_6, DMSO-d_6 and D_2O to ascertain the effect of self-association in different solvents (Figs. 2A–C). Coralyne molecule contains 22 protons (Fig. 1), comprising seven aromatic protons, one methyl and four methoxy (OCH_3) groups [27]. Since the proton signals in D_2O at 25 °C were broad, presumably due to self-association (discussed later), we also recorded the spectra in D_2O at 40 °C (Fig. 2D). 1D ^{1}H NMR spectra show 2 doublets and 5 singlets (2 of them overlap in D_2O) in the aromatic region, 4 singlets at 3.5–4.2 ppm and 1 singlet at 2.6–3.5 ppm (Figs. 2A–D). H6 and H5 protons are located three bonds away from each other and appear as doublets at 8.05 and 7.26 ppm in D_2O at 40 °C (Fig. 2D). This is confirmed by observed vicinal coupling constant $^{3}J = 7.40$ Hz as well as the observed cross peak in $^{1}H-^{1}H$ COSY spectra (Fig. S1). H6 proton is located two bonds away from the positively charged nitrogen atom in isoquinoline ring of coralyne, while H5 proton is three bonds away, so that the resonance, which is relatively shifted downfield at 8.05 ppm, is assigned to H6 proton and that at 7.26 ppm is assigned to H5 proton. The resonance at 2.81 ppm is straight away assigned to $16CH_3$ protons (Fig. 2D). The 5 singlets at 6.6–7.9 ppm and 4 singlets at 3.7–4.0 ppm in spectra acquired in D_2O solvent (Fig. 2D) refer to H1, H4, H9, H12, H13 and $2OCH_3$, $3OCH_3$, $10OCH_3$, and $11OCH_3$ protons, respectively. Their specific assignment was done on the basis of 2D $^{1}H-^{1}H$ ROESY spectra (Figs. 3A and B), showing several NOE correlations (Table S1) having relative intensity of the NOE cross peaks designated as very strong (ss), strong (s), medium (m) and weak (w) corresponding to approximate range of distances as <2.5, 2.5–3.5, 3.5–4.0, and >4.0 Å, respectively. Since coralyne aggregates, leading to line broadening of aromatic proton signals, the ROESY spectra were recorded at 40 °C. H6 is found to give intense cross peak with H5 proton, which is 3 bonds away from it. $16CH_3$ gives NOE cross peak of very strong (ss) intensity with H6 proton and a weak (w) intense NOE cross peak with H5, which is farther away from $16CH_3$ as compared to H6. It also gives a NOE cross peak of very strong intensity with a resonance at 6.80 ppm which gets

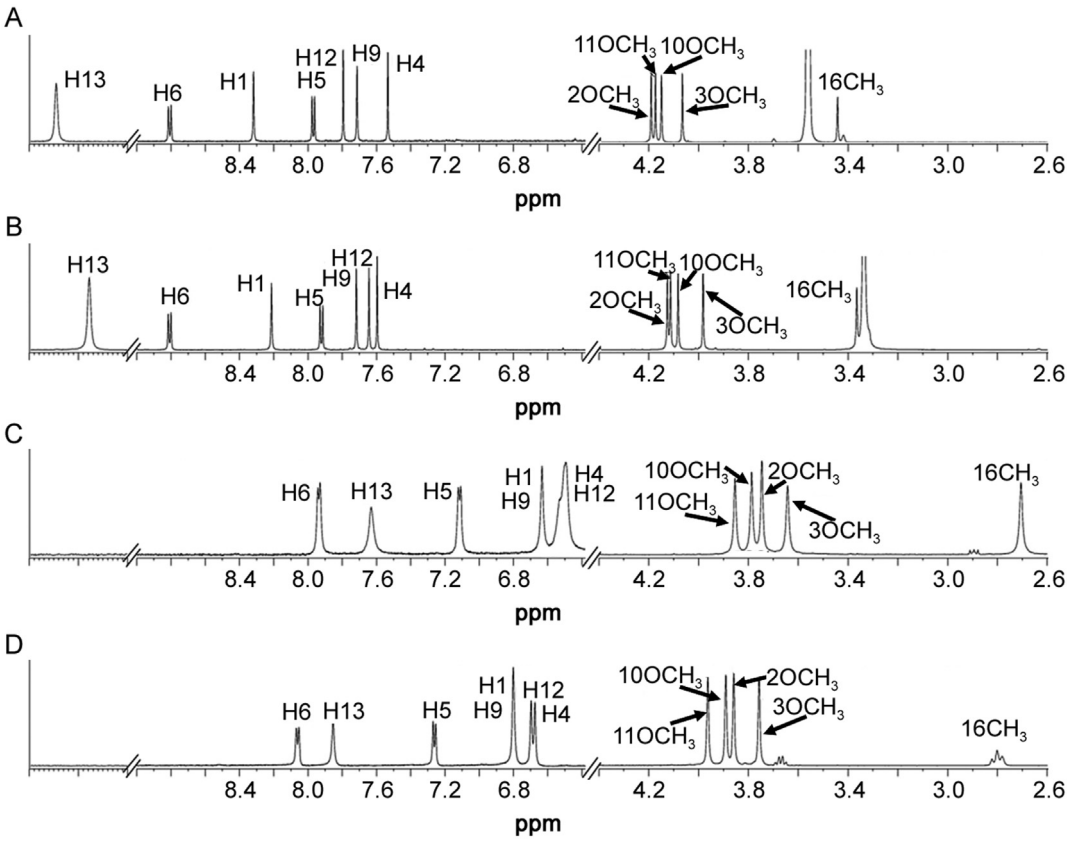

Fig. 2. 1D ^{1}H NMR spectra of (A) 8.0 mM coralyne in ethanol-d_6 at 25 °C, (B) 11.0 mM coralyne in DMSO-d_6 at 25 °C, (C) 3.17 mM coralyne in D_2O at 25 °C and (D) 3.17 mM coralyne in D_2O at 40 °C.

assigned to H9 proton. H9 gives a very intense (ss) NOE cross peak with one of the methoxy groups (OCH_3) resonating at 3.88 ppm which is thus assigned to $10OCH_3$. H5 gives a very strong intensity (ss) NOE cross peak with a resonance at 6.67 ppm which gets assigned as H4. H4 gives a very strong (ss) NOE cross peak with a signal resonating at 3.75 ppm which gets assigned as $3OCH_3$. The singlet resonating at 7.85 ppm gives a very strong (ss) intensity cross peak with two singlets at 6.80 and 6.69 ppm but does not give NOE cross peak with any of the methoxy protons. On the contrary, signals at 6.80 and 6.60 ppm give very strong (ss) NOE cross peak with signals at 3.85 and 3.96 ppm, respectively. Thus the signal at 7.85 ppm gets assigned to H13 proton and the other two singlets resonating at 6.80 and 6.69 ppm are assigned to H1/H12 protons (Fig. 1). The relatively more downfield shifted resonance at 6.80 ppm is assigned to H1 since it is four bonds away from N^+ atom, while that at 6.69 ppm, which is five bonds away from N^+, is assigned to H12 proton. Accordingly, the resonances at 3.85 and 3.96 ppm, which give very intense (ss) cross peaks with resonance at 6.80 and 6.69 ppm, are assigned to $2OCH_3$ and $11OCH_3$, respectively. The unambiguous assignment of all protons is shown in Table 1. In a similar way we could assign all protons of coralyne in DMSO-d_6 and ethanol-d_6 (Table 1), using ^{1}H–^{1}H ROESY spectra recorded in these solvents (Figs. S2 and S3). It may be noted that besides these 11 intra molecular NOE correlations (serial no. 1–11 in Table S1), 3 other NOE correlations were found to exist in D_2O solvent (serial no. 12–14 in Table S1 and marked as star symbol in Figs. 3A and B), which are discussed later in Section 3.3. It may be noted that the present studies are the first report of assignment of each and every proton in NMR spectra in 3 different solvents. Earlier studies in literature have reported [16] assignment of only aromatic protons, which are comparable to that obtained in present work (Table S2).

Each of the aromatic proton resonances, that is, H1, H4, H5, H6, H9, H12 and H13, gives cross peak with a single carbon resonance in the range 100–125 ppm in ^{1}H–^{13}C HSQC spectra in D_2O (Fig. S4A), that is, the region of aromatic carbon resonances. Since all proton resonances are already assigned, we directly get assignment of respective carbon atoms to which they are attached, that is, C1, C4, C5, C6, C9, C12 and C13 (Tables 2 and S3). $2OCH_3$, $3OCH_3$, $10OCH_3$ and $11OCH_3$ protons show single bond correlation with four carbons resonating in the range of 55–60 ppm and therefore are assigned to respective carbons, that is, C14, C15, C17 and C18, respectively (Fig. S4B). $16CH_3$ protons are attached to carbon signal resonating in the range 15–18 ppm, which is assigned to C16 (Fig. S4C). Thus, the assignment of all carbons directly attached to protons was accomplished (Tables 2 and S3) from the observed ^{1}H–^{13}C HSQC correlations. The carbons directly attached to protons in ethanol-d_6 and DMSO-d_6 were assigned in a similar way (Tables 2 and S3) using ^{1}H–^{13}C HSQC spectra recorded in these solvents (Figs. S5A–C, S6A-C).

In DMSO solvent, we were able to record ^{1}H–^{13}C HMBC spectra (Figs. 4A and B), which enabled us to assign all other carbon atoms using standard methodolgies of ^{1}J, ^{2}J and ^{3}J couplings of protons from their neighbouring carbons, which are 1, 2 and 3 bonds away, respectively (Tables 2 and S3). For example, H13 splits into two cross peaks symmetrically about its position at 9.58 ppm (Fig. 4A) due to ^{1}J with C13 resonating at 116.54 ppm, as inferred from ^{1}H–^{13}C HSQC spectra (Fig. S5A). It also shows ^{2}J coupling with C12a,

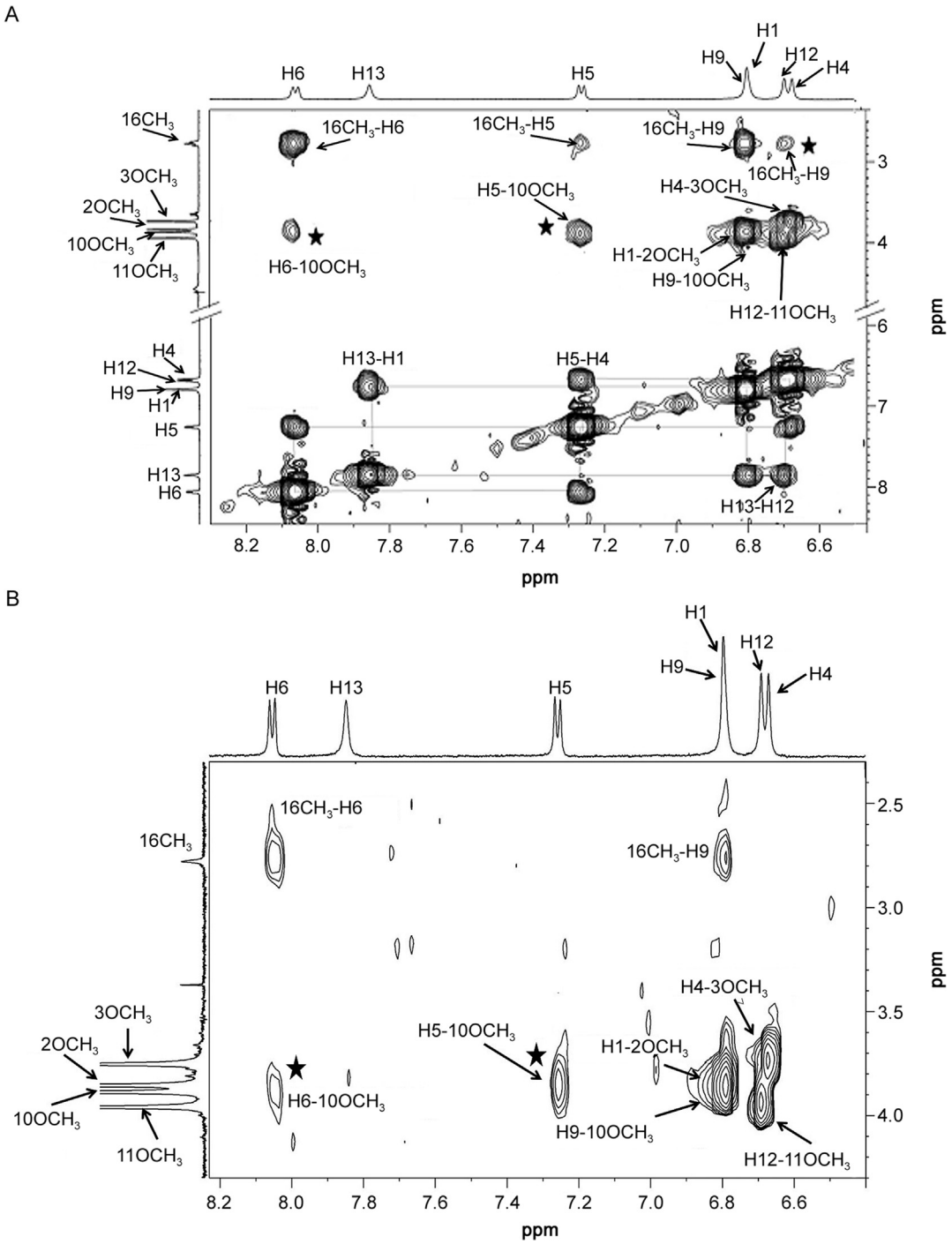

Fig. 3. (A) Expansion of specific region of 2D $^{1}H-^{1}H$ ROESY spectra of 3.17 mM coralyne in D_2O at 40 °C indicating the observed NOEs. Star symbol indicates inter-molecular NOEs in the structure of coralyne dimer as discussed in Section 3.3. (B) Expansion of part of NOESY spectra showing four methoxy groups resolved separately.

C13a and ^{3}J coupling with C8a, C12, and C13b (Fig. 4A**,** Table S3). Each methoxy proton gives ^{3}J coupling with carbon resonances in the range 151–160 ppm, which get assigned to their corresponding C2, C3, C10, and C11 aromatic ring protons (Fig. 4B**,** Table S3). The methyl protons resonating at 3.37 ppm give ^{2}J and ^{3}J couplings with C8 and C8a, respectively so that carbon resonances at 145.71 and 122.38 get assigned to C8 and C8a, since C8a is expected to be downfield shifted, being in the proximity of N atom at 7^{th} position (Fig. 1). In a similar way it was found that all protons assigned already (Table 1) were coupled through ^{1}J, ^{2}J and ^{3}J spin-spin couplings with respective carbon resonances (Table S3) in the HMBC spectra (Figs. 4A and B) and were thus assigned unambiguously (Table 2). We have thus obtained assignment of each and every carbon signal in the NMR spectra in DMSO solvent for the first time.

3.2. Chemical shift calculations

The theoretical ^{13}C and ^{1}H chemical shifts of coralyne were calculated by subtracting the absolute shielding of each atom with

Table 1
Chemical shifts (δ) of coralyne protons (^{1}H) obtained from NMR spectra in different solvents, D_2O (40 °C), DMSO-d_6 (25 °C), ethanol-d_6 (25 °C) and their comparison with that calculated in gas and ethanol phase using wave functions by GAIO method using B3LYP method.

Proton	Experimental δ (ppm)			Theoretical δ (ppm)	
	D_2O	DMSO-d_6	Ethanol-d_6	3-21G ethanol phase	6-311G** gas phase
H1	6.80	8.22	8.31	8.02	8.33
H4	6.67	7.60	7.53	6.87	7.18
H5	7.26	7.94	7.96	7.83	7.75
H6	8.05	8.82	8.80	8.35	8.16
H9	6.80	7.73	7.71	6.73	7.22
H12	6.69	7.65	7.79	7.07	7.17
H13	7.85	9.58	9.64	8.94	8.97
$2OCH_3$	3.85	4.13	4.19	4.84	4.74
$3OCH_3$	3.75	3.99	4.06	4.80	3.87
$10OCH_3$	3.88	4.09	4.14	4.31	3.91
$11OCH_3$	3.96	4.12	4.17	4.39	3.99
$16CH_3$	2.81	3.37	3.44	3.05	2.77

respect to that of Tetra Methyl Silane (TMS). The basis set used to calculate the absolute shielding of ^{13}C and ^{1}H in TMS by B3LYP method was the same as the ones employed for coralyne. Absolute shielding of ^{13}C was 184.43 in gas phase using 6-311G** basis set and 203.21 for ethanol using 3-21G basis set. Absolute shielding of ^{1}H was 32.0 in gas phase using 6-311G** basis set and 32.93 for ethanol using 3-21G basis set. The theoretical and experimental chemical shifts of ^{1}H and ^{13}C are shown in Tables 1 and 2, respectively. Analysis of the results revealed that the chemical shifts are sensitive to change in phase from gas to ethanol. Chemical shifts are prone to vary with chemical environment like interactions with solvent and molecular conformation. Therefore, we have determined the linear correlation between the experimental ^{1}H and ^{13}C chemical shifts in DMSO solvent and corresponding calculated chemical shift values in gas phase (Figs. S7A and C). The correlation in ethanol solvent is also shown (Figs. S7B and D). The plots showed linear correlation coefficient of 0.96–0.98 for ^{1}H (Figs. S7A and B) and 0.99 for ^{13}C chemical shift values, respectively (Figs. S7C and D). It may be noted that in ethanol solvent, chemical shift values of quarternary carbons could not be obtained since coralyne does not give a good 1D^{13}C and 2D ^{1}H–^{13}C HMBC spectra in ethanol. Inspite of the fact that we obtained the ^{13}C chemical shift for only those carbons which are attached to protons from ^{1}H–^{13}C HSQC spectra and not all ^{13}C atoms, the correlations in ethanol solvent are found to be good. Although we have performed calculations for a limited basis set, the results are encouraging as they correlate well with experimental results on a scale of 1.0. The findings are the first attempt to calculate all ^{1}H and ^{13}C chemical shifts. The optimized structure of coralyne in gas and ethanol phase using B3LYP method is shown (Figs. 5A and B).

3.3. Self-association - NMR experiments

We observed that the proton resonances in water are shifted significantly upfield (Figs. 2C and D and Table 1), up to 1.7 ppm, with respect to that in ethanol and DMSO (Figs. 2A and B and Table 1). It has been independently established that coralyne does not aggregate in DMSO and 100% ethanol [16,20]. Therefore, the chemical shift positions in 100% ethanol or DMSO have been considered to be due to monomer form of coralyne [16]. The relatively small difference in chemical shifts in different solvents (ethanol/DMSO) is expected due to difference in susceptibility or inter-molecular associations (Figs. 2A and B). The observed upfield shift in water may be attributed to self-association of coralyne [16,28]. We recorded 1D ^{1}H NMR spectra of coralyne in D_2O at 40 °C with and without addition of salt (Figs. 6A and B). We observed that in the presence of 120 mM K^+ (Fig. 6A), all resonances are further upfield shifted, the shift being maximum ~0.5 ppm for H1 and H13 protons (Table S4). This is in accord with the observation that salt promotes self-association [18].

In order to get a direct insight into self-association of coralyne, we recorded ^{1}H NMR spectra of coralyne as a function of concentration under no salt condition (Fig. 7). It is observed that all aromatic protons shift upfield with concentration to a larger extent (Figs. 7, S9a and Table S5). The shift is maximum for H1 proton (1.17 ppm), followed by H13 and H12 protons which shifted upfield by ~0.90 and 0.88 ppm, respectively. The methyl and methoxy protons also show large upfield shift with concentration by ~0.34–0.42 ppm. We find that the chemical shift of all protons of the lowest concentration of coralyne sample examined by us by NMR, that is 0.05 mM, are upfield shifted as compared to that in DMSO and ethanol (e.g. H13 proton by 1.2 ppm, Table 1) which are presumably that of monomer coralyne. This suggests that self-association exists to a considerable extent at 50 μM concentration even in the absence of salt, as confirmed independently by fluorescence lifetime measurements (55 μM) discussed later in Section 3.4. Several groups of workers have demonstrated occurrence of upfield shifts due to stacking of aromatic rings on formation of dimers or higher order aggregates in anthracycline/anthraquinone/fused ring compounds [28–35]. The NMR spectra of aggregated form of coralyne (3.17 mM concentration) with temperature show downfield shift in all proton resonances to different extents (Figs. S8 and S9B and Table S6). The increase in temperature diminishes the stacking interactions and does not favor formation of aggregates [16,28]. The shift in H13, H1 and H12 protons is large, 0.44–0.53 ppm (Table S6), which is consistent with that observed on decrease of concentration [28] (Table S5).

We observed 14 NOE correlations due to short distance contacts between coralyne protons obtained from ^{1}H–^{1}H ROESY at mixing time, $\tau_m = 200$ ms at 40 °C (Table 3) of which 11 NOEs (Table S1) are due to intra molecular short contacts, as discussed in Section 3.1. The ROESY spectra recorded in the absence of any salt presumably refer to that of dimer and not higher aggregates. Our argument is supported by the observation that dimer is the dominant species in mass spectrometry experiments performed with 5 mM aqueous solution of coralyne [16]. The distances corresponding to all NOEs are calculated using distance between H5 – H6 protons (2.44 Å) as a reference (Table 3). García and co-workers have earlier reported existence of 4 NOE correlations, among aromatic protons in their study using 2D ^{1}H–^{1}H ROESY spectra [16]. The distances corresponding to these NOEs, that is, H6 – H5 = 2.42 Å, H13 – H1 = 1.93 Å, H5 – H4 = 2.47 Å, and H12 – H13 = 2.45 Å, are comparable to our findings (Table 3). All other short contacts involve methyl and methoxy protons, which were not shown in their NMR

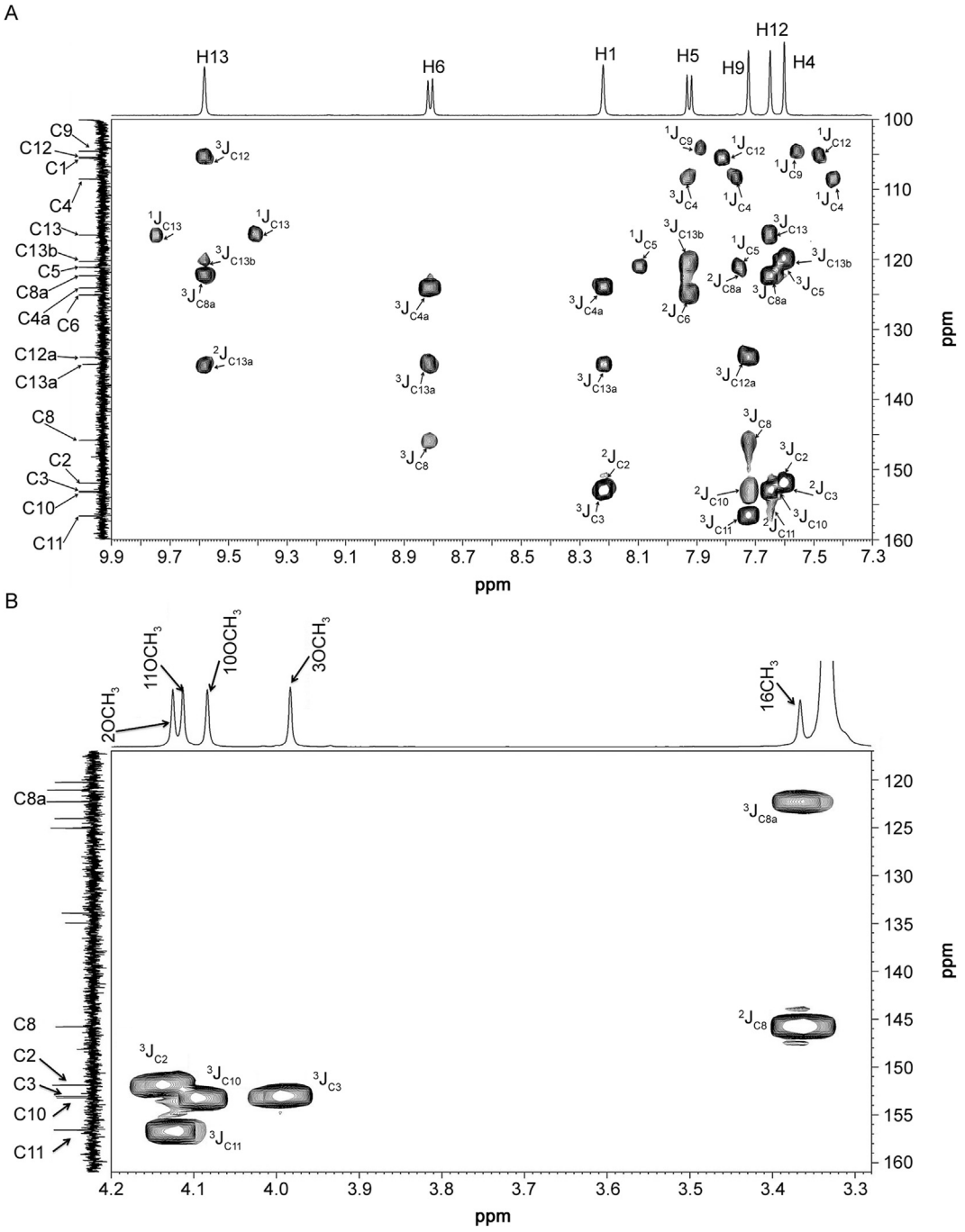

Fig. 4. (A) and (B) Expansions of specific regions of $^{1}H-^{13}C$ HMBC spectra of 11.0 mM coralyne in DMSO at 25 °C showing proton and carbon atoms having one, two and three bond $^{1}H-^{13}C$ spin-spin couplings (^{2}J, ^{3}J and ^{4}J).

experiments.

We have built a model of coralyne molecule using INSIGHT II with its rings A, B, C and D in a plane and methoxy groups oriented freely in different ways. We find that the calculated distances corresponding to NOE correlations listed in S. No. 1–11 in Table 3 indeed pertain to intra molecular short distance contacts in coralyne molecule. However, the distances of H5, H6 and H12 protons from $10OCH_3$, $10OCH_3$ and $16CH_3$ protons, respectively corresponding to NOE correlations listed in S. No. 12–14 in Table 3 are 11.3, 8.3 and 6.5 Å in this structure built by using 11 intra molecular NOEs. We built a molecular structure of single coralyne molecule (Fig. 1) using INSIGHT II and found that the distances corresponding to these NOEs (S. No. 12–14) indeed lie in the range 6–12 Å. Therefore, these 3 NOE correlations cannot be intra molecular and pertain to two different molecules of coralyne in the vicinity of each other, hereafter referred to as inter-molecular NOEs. We then built a model of coralyne dimer with their aromatic planar rings stacked over each other in a head to tail arrangement, that is, two rings placed practically anti-parallel to each other and introduced all experimentally observed inter proton distance restraints (Table 3),

Table 2
Chemical shifts (δ) of carbon resonances (^{13}C) of coralyne obtained from NMR spectra in different solvents, D_2O (40 °C), DMSO-d_6 (25 °C), ethanol-d_6 (25 °C) and their comparison with that calculated in gas and ethanol phase using wave functions by GAIO method using B3LYP method.

Carbon	Experimental δ (ppm)			Theoretical δ (ppm)	
	D_2O	DMSO-d_6	Ethanol-d_6	3-21G ethanol phase	6-311G** gas phase
C1	102.61	105.41	105.65	101.63	118.22
C2	–	151.94	–	139.28	161.13
C3	–	153.06	–	140.56	160.79
C4	106.86	108.39	108.4	100.60	113.17
C4a	–	124.19	–	109.65	127.85
C5	120.7	120.97	122.32	110.92	128.02
C6	122.68	124.97	121.10	111.09	125.09
C8	–	145.71	–	129.24	145.93
C8a	–	122.38	–	109.73	127.70
C9	102.61	104.47	103.98	94.50	105.05
C10	–	153.15	–	142.28	163.41
C11	–	156.69	–	144.86	166.52
C12	103.78	105.41	105.65	97.05	107.86
C12a	–	134.05	–	117.60	138.66
C13	114.18	116.54	117.32	105.69	120.34
C13a	–	135.11	–	121.52	140.10
C13b	–	120.40	–	109.0	126.77
C14	56.45	57.09	57.11	55.36	58.69
C15	55.98	56.55	56.82	53.94	57.41
C16	16.60	17.92	16.12	17.63	18.23
C17	56.45	56.96	57.11	54.45	57.95
C18	56.87	57.06	57.11	60.29	64.10

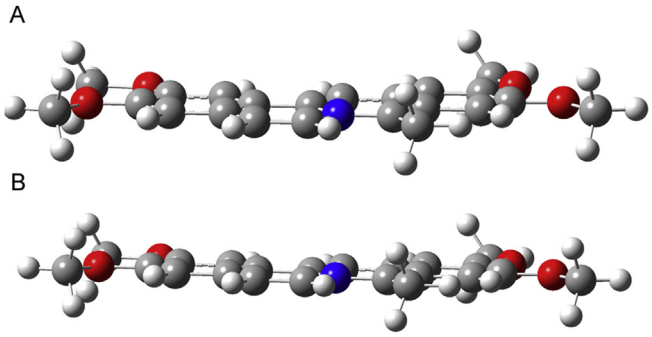

Fig. 5. Gaussian optimized structure of coralyne in (A) gas phase and (B) ethanol phase.

that is, 3 inter-molecular NOEs (S. No. 12–14) apart from 11 intra molecular NOEs (S. No. 1–11). The structure obtained after restrained energy minimization and molecular dynamics simulations is shown in Figs. 8A and B. The various intra- and inter-molecular distances in the dimer structure obtained (Table 3) are found to agree reasonably well with the calculated distances from intensity of NOE cross peaks. It may be noted that nitrogens lie in the centre of the aromatic rings so that the cation-pi interaction may have a role to play apart from dominant stacking interactions between aromatic rings of 2 molecules of coralyne in the stacked dimer.

We have used ^1H chemical shift data as a function of concentration and temperature to obtain dimerization constant and thermodynamic parameters. The dimerization constant (K_D) was calculated using the following equation [33]:

$$K_D = \frac{C_D}{C_M^2} \quad (2)$$

$$K_D = \frac{C_T - C_M}{2C_M^2} \quad (3)$$

where C_T is the total concentration of coralyne, C_M is the monomer concentration and C_D is the dimer concentration. Accordingly, the plot of observed chemical shift as a function of concentration (Fig. S9A) for H13 proton, fits into a curve obtained from the following relation, given by Davies et al. [35]:

$$\delta = \delta_M + (\delta_D - \delta_M)\left(\frac{4K_DC_T + 1 - \sqrt{8K_DC_T + 1}}{4K_DC_T}\right) \quad (4)$$

where δ is the observed chemical shift (ppm), δ_M is the chemical shift of monomer (ppm) and δ_D is the chemical shift of dimer (ppm). The estimate of dimerization constant for H13 proton is $K_D = 0.5 \times 10^3\ M^{-1}$. Using indefinite non-cooperative association model [35], the estimate obtained is $K_D = 1 \times 10^3\ M^{-1}$. The dimerization constant at different temperatures was calculated using the data on temperature dependence of chemical shift (Fig. S9B). Accordingly the thermodynamic parameters were calculated using the following equation:

$$\ln\ (K_D) = \left(\frac{\Delta S}{R}\right) - \frac{\Delta H}{RT} \quad (5)$$

where ΔH is change in enthalpy, ΔS is change in entropy, R is universal gas constant and T is the temperature. The thermodynamic parameters for H13 proton using dimer model are $\Delta H = -10.8$ kcal/mol and $\Delta S = -23.9$ cal deg^{-1} $mole^{-1}$. The corresponding values for indefinite non-cooperative association model are found to be much higher. Since our observed intra- and inter-molecular inter proton distances from ROESY spectra agree with that obtained from restrained molecular dynamics simulations, we believe that a dimeric form of coralyne exists predominantly in solution in the absence of salt and an oligomeric form leading to indefinite association does not exist. Such a dimer structure (Fig. 8) in which aromatic rings of two molecules are stacked and overlap considerably is expected to lead to a decrease in enthalpy by 10–13 kcal/mol

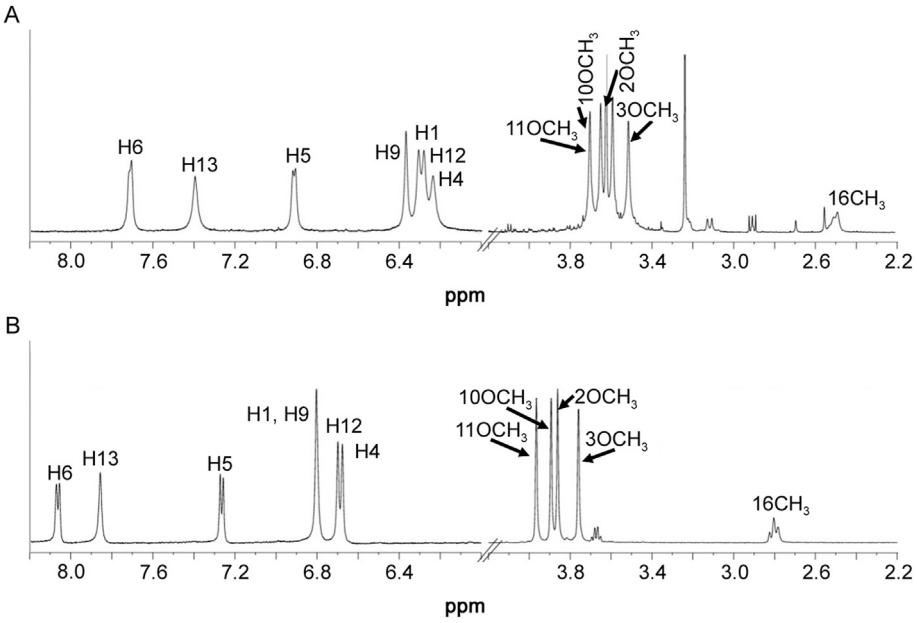

Fig. 6. Proton NMR spectra of 3.17 mM coralyne in D_2O (A) with 120 mM K^+ and (B) without salt at 40 °C.

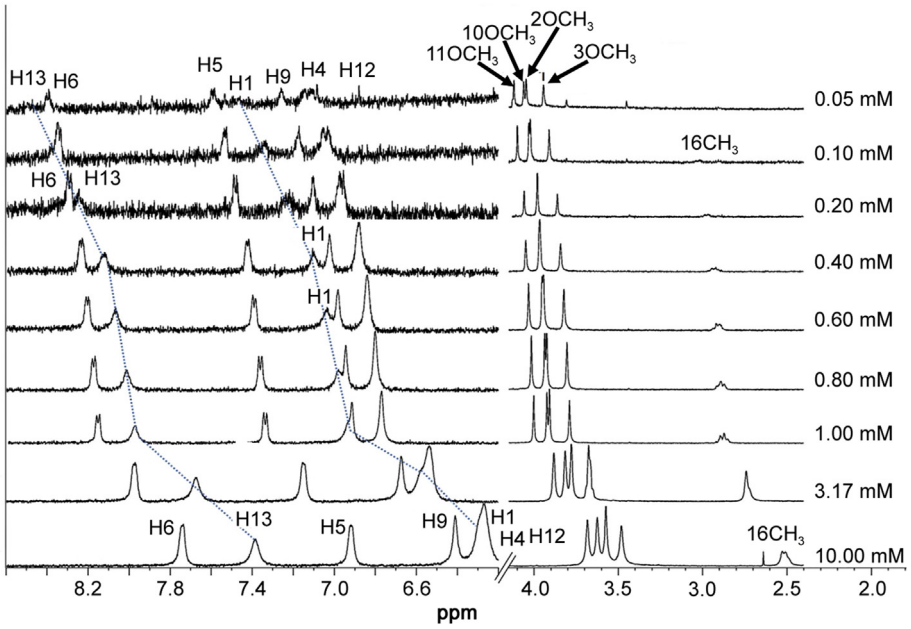

Fig. 7. Proton NMR spectra of coralyne in D_2O at different concentrations in the range 0.05–10.0 mM at 25 °C with no added salt.

which is typical of stacking interactions [28–35]. The observed $\Delta H = -10.8$ kcal/mol and $\Delta S = -23.9$ cal deg^{-1} $mole^{-1}$ corroborate formation of ordered stacked dimer, which would result in decrease of both enthalpy and entropy. Our findings are further supported by the results of mass spectroscopy experiments which reveal that most abundant aggregated compound in 5 mM aqueous solution of coralyne is the dimer species [16]. The values of dimerization constant and thermodynamic parameters obtained are of the same order as that reported in literature [16].

3.4. Self-association - optical spectroscopy experiments

Absorption spectra of coralyne were recorded in ethanol, DMSO and water (concentration = 14–22 μM) at 25 °C (Fig. 9A). The spectra in ethanol and DMSO clearly show absorption maxima at 284, 301, 313, 328, 363, 406 and 428 nm. The aqueous solution appears to have coralyne in aggregated form resulting in lower absorption at 310 nm as compared to 300 nm as well as broadening of 405 and 420 nm peak into a single peak [16,18,19]. Since DNA binding experiments are generally performed at physiological salt

Table 3
Inter proton distances within coralyne calculated from intensity of cross peaks in 2D ^{1}H–^{1}H ROESY spectra in D_2O at 40 °C and the same observed in structure obtained by restrained Molecular Dynamics (rMD) simulations. O denotes overlap of the NOE cross peaks.

S. No.	NOE correlation	Inter proton distances (Å)	
		From NOE cross peak	From rMD structure
	Monomer (intramolecular)		
1	H6 – H5	2.44	2.37
2	H13 – H1	2.32	2.10
3	H5 – H4	2.47	2.45
4	H12 – H13	2.67	2.41
5	H6 – 16CH_3	2.34	2.64
6	H9 – 16CH_3	2.49	2.69
7	H5 – 16CH_3	4.22	4.27
8	2OCH_3 – H1	2.14 (O)	2.69
9	3OCH_3 – H4	2.12 (O)	2.44
10	10OCH_3 – H9	2.14 (O)	2.62
11	11OCH_3 – H12	2.12 (O)	2.44
	Dimer (intermolecular)		
12	H6 – 10OCH_3	3.94	4.10
13	H5 – 10OCH_3	3.14	3.00
14	H12 – 16CH_3	4.18	4.20

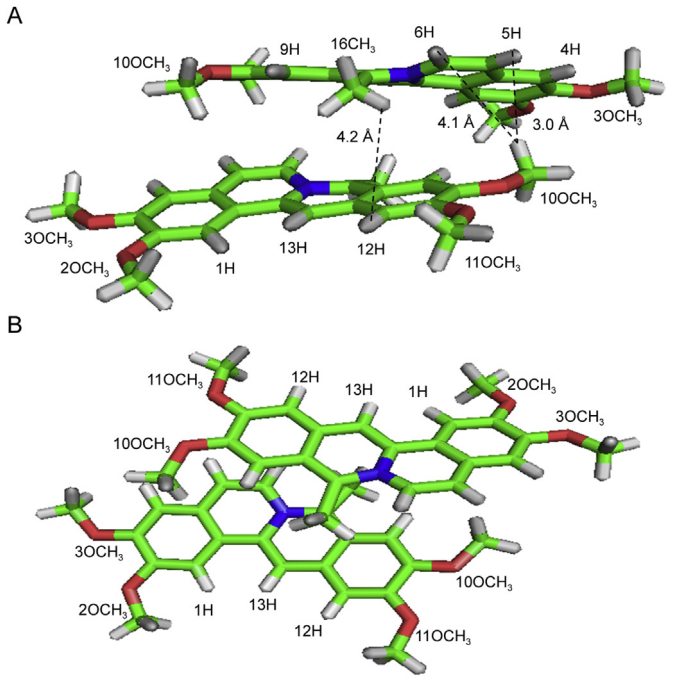

Fig. 8. (A) and (B) Structure of self-associated stacked dimer having two molecules of coralyne in head to tail anti-parallel orientation based on rMD simulations using experimental distance restraints from ^{1}H–^{1}H ROESY spectra in different orientations.

concentration, we recorded the absorption spectra of coralyne in aqueous solution as a function of concentration in the range 1–40 μM, with salt concentration $K^+ = 120$ mM (Fig. S10A) and in the absence of salt (Fig. S10B). We observed isobestic point at 431 and 330 nm in aqueous solution (Fig. S10B) indicating existence of two species, that is, monomeric form of coralyne along with the same in aggregated form. In presence of 120 mM K^+ isobestic point at these wavelengths is not observable (Fig. S10A) and there may be a possibility of formation of higher order aggregates. This is in agreement with the results reported earlier [18] that presence of salt promotes self-association. Fluorescence spectra recorded in aqueous solution as a function of concentration at 25 °C show increase in emission intensity (F) with concentration in the range 0.2–1.8 μM (Fig. 9B, Figs. S11A and B). The relative fluorescence quantum yield (ϕ_F) decreased with concentration (Fig. S11C), which may be due to weaker emission of dimer formed at higher concentration as reported earlier [19]. In order to examine self-association of coralyne, we recorded the CD spectra of 3.1 and 30.0 μM coralyne in aqueous solution (Fig. S11D). The corresponding absorbance spectrum has been overlaid to examine if bisignate bands [32] centered at absorption maxima exist (Fig. S11D). CD spectra of 30.0 μM coralyne in aqueous solution in presence of salt show several CD bands which could be a combination of negative and positive bisignate bands centered at several absorption maxima, 282, 296, 310, 323, 360, 405 and 420 nm in a short range of wavelength. It was not possible to arrive at a specific conclusion regarding aggregation. No such CD bands were observed for coralyne in the absence of salt even at milli molar concentration.

Time resolved fluorescence measurements showed exponential decay (Fig. 9C) with an average lifetime (τ_1) of 9.4 ns in the concentration range 0.04–1190 μM in aqueous solvent in the absence of salt (Table S7). When the concentration was raised to 2.0 μM, a long lived fluorescence component with a lifetime $\tau_2 = 22.7$ ns appeared with a relative abundance (α_2) of 10.5% which gradually increased in amplitude with concentration (Table S7). This component has earlier been attributed to formation of dimer [19]. It has been shown by mass spectrometry experiments that the most abundant aggregated compound at 5 mM coralyne in aqueous solution is a dimer [16]. Emission with longer lifetime suggests that dimer formation reduces the radiative transition of the singlet excited state, resulting in lower quantum yield, as proposed earlier [19]. In the presence of salt, the average value of lifetime was $\tau_1 = 8.8$ ns for the monomer form and $\tau_2 = 30.7$ ns for the aggregated form (Table S7) and dimerization constant evaluated [33] using equation (3) is $K_D = 4.5 \times 10^3$ M^{-1}.

4. Discussion

We have obtained complete assignment of all aliphatic and aromatic protons in ethanol-d_6, DMSO-d_6 and D_2O for the first time. García et al. [16] have reported assignment of only aromatic protons in ethanol-d_6, DMSO-d_6 and D_2O, which are comparable to that reported here. Slight observed differences (Table 1) may be due to presence of 5.0 mM NaCl salt used in their experiments. Hazra et al. [17] have reported assignment of only aromatic protons and their proximity to cyclodextrins on binding. ^{13}C NMR chemical shifts of coralyne have not been reported in literature so far and the present study is the first one in this context. Further, to the best of our knowledge, there is no study on computation of chemical shifts of coralyne reported so far in literature. On the whole, the obtained results from present study demonstrate the application of B3LYP exchange-correlation function using 3-21G and 6-311G basis sets in prediction of NMR chemical shifts, which agree reasonably well with experimental results. The assignment of each and every proton and several carbon-13 resonances can now be used for determining role of methyl and methoxy groups, besides the aromatic protons, in binding to nucleic acids. The carbon-13 chemical shifts become very handy in assignment of protons in NMR spectra of coralyne complexed to DNA through ^{1}H–^{13}C HSQC spectra [21].

Several DNA intercalating drugs such as daunomycin [28,29], mitoxantrone [30,33], actinomycin [34,35], and proflavin [36], consisting of conjugated aromatic rings are known to form aggregates by self-association. Initial increase of concentration of these compounds leads to formation of dimers. Presence of 2 species in equilibrium is characterized by isobestic point in absorption and fluorescence spectra. At higher concentration, these compounds having 3 or more planar aromatic rings may associate to higher aggregated forms by continuous stacking of aromatic rings and

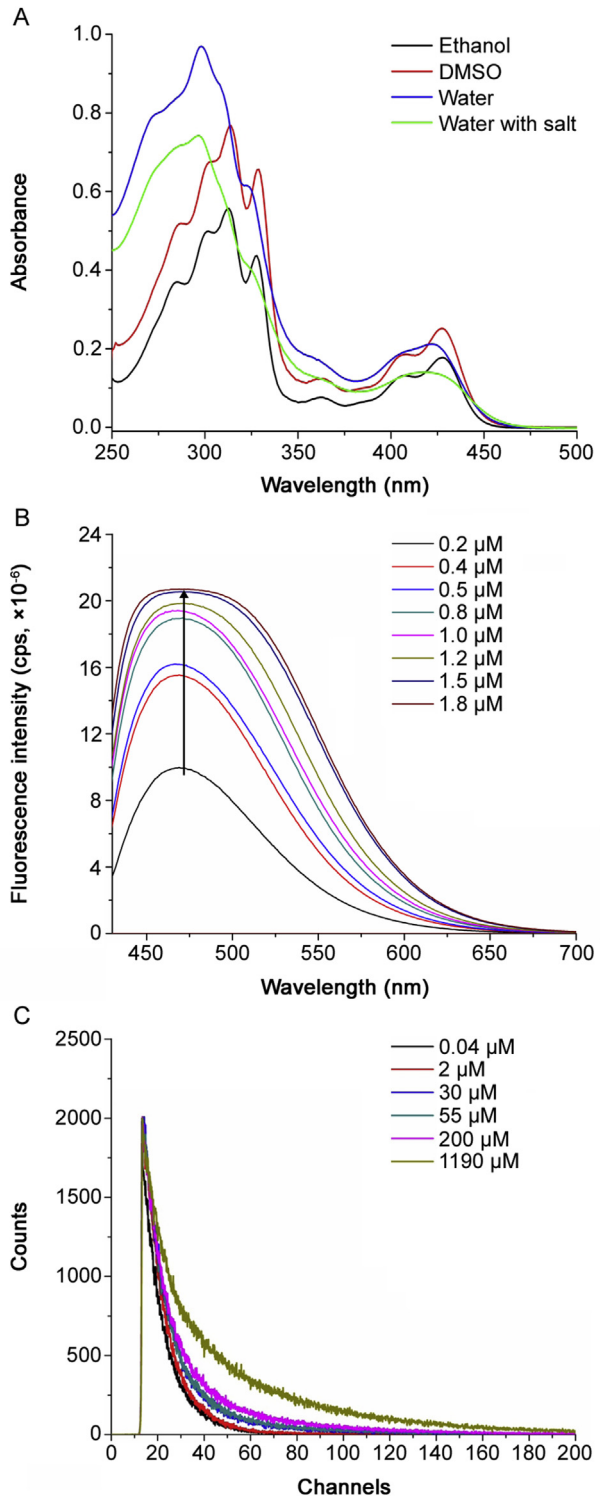

Fig. 9. (A) Absorption spectra of coralyne in different solvents at 25 °C. The concentration of coralyne in DMSO, ethanol, water and water containing 120 mM K^+ salt was 22.4, 13.6, 14.7 and 15.0 μM, respectively. (B) Fluorescence spectra showing relative emission intensity (cps, counts per sec) of coralyne in water at different concentrations at 25 °C; arrow indicates increase in concentration. (C) Fluorescence lifetime decay of coralyne at different concentrations in aqueous solution in the absence of salt at 25 °C.

isobestic point is lost [28]. Our results by absorption spectroscopy show that coralyne is present in monomer form in DMSO and ethanol. In water, presence of isobestic point indicates formation of two species whereas in presence of 120 mM K^+, higher aggregates may exist. These are in agreement with the reports in literature that salt induces aggregation [16,18,19]. In the absence of salt, the fluorescence spectra in water are similar to that reported in literature [19] wherein it has been shown that existence of monomer and dimer in equilibrium can explain experimental results. Fluorescence lifetime measurements confirmed existence of a dimer having long lived lifetime (τ) value.

NMR experiments show that proton resonances in water are upfield shifted as compared to that in DMSO and ethanol (Figs. 2A and B). Concentration dependent upfield shifts have been interpreted as a proof of stacking interactions in self-associated structures [16,29,35]. However, the upfield shifts in aqueous solution are much more in presence of 120 mM K^+ (Fig. 6, Table S4) as salt induces self-association [18]. The agreement between distances calculated from intensity of 3 inter-molecular NOEs and the corresponding distances in rMD structure, give an independent and direct conclusive evidence of formation of dimer in aqueous solution in the absence of salt. The orientation of two molecules in the structure of dimer (Fig. 8) shows that maximum shielding occurs for H1 and H13 protons, which would be most upfield shifted on stacking of aromatic rings A, B, C and D of two coralyne molecules. Using iso-shielding curves [37], the calculated upfield shifts of H13 and H1 protons are ~1.0 ppm, which match with the observed large upfield shifts of ~0.9–1.2 ppm in H13 and H1 protons. NMR based structure of dyes [29,38] has shown that inverted stack type of association is favored by these molecules, which may be a general feature of self-association of planar aromatic compounds. We observe that the aromatic rings A, B, C and D of two molecules of coralyne are in anti-parallel orientation with respect to each other, but are also somewhat laterally displaced (Fig. 8), which may occur as an alternate way to minimize charge repulsion between N^+ atoms on each molecule. Our NMR results therefore establish formation of dimer in 3.17 mM aqueous solution of coralyne. Higher aggregates may be present in the presence of salt. The NMR based results are in agreement with the findings by mass spectrometry which revealed [16] that the most abundant aggregated compound in 5 mM aqueous solution of coralyne in the absence of any salt is the dimer species.

5. Conclusions

Coralyne exists in monomer form in DMSO and ethanol. Self-association occurs in water in the presence or absence of salt. In the absence of salt, 3.17 mM coralyne in aqueous solution has dominant aggregated form as dimer with 2 molecules of coralyne stacked over each other in anti parallel orientation but displaced spatially with respect to each other. Dimer formation is independently proved by the fluorescence lifetime measurements and other techniques. All proton and several carbon-13 chemical shifts in NMR spectra of coralyne have been unambiguously established. Coralyne is known to have anti-leukemic activity [7,8] and targets different forms of DNA [10–14]. Binding of coralyne, in monomer and dimer states, to different structural forms of nucleic acids including non-canonical forms, can be evaluated using NMR techniques. The observed chemical shifts including those of carbon-13 are particularly useful when the overlap and broadening of resonances due to binding occurs and creates a problem in spectral assignments [21] as well as ascertaining inter-molecular NOE cross peaks between ligands and DNA. The findings thus have direct application in quantitative as well as structural analysis of interaction of coralyne with nucleic acids or other bio-receptors like polysaccharides [19] for the purpose of structure based drug designing.

Acknowledgments

The author K. Padmapriya would like to thank Ministry of Human Resources and Development (MHRD), Government of India for the support for funding. The facilities provided by the Central NMR Facility, Indian Institute of Technology Roorkee, Uttarakhand, India are highly acknowledged. The authors are thankful to Mr. Akhada Sri Teja for help in carrying out mathematical calculations. The authors are also thankful to Dr. Kumud Pandav, Dr. Zia Tariq and Ms. Shailja Raje for help in making figures.

Conflicts of interest

Authors declare that there are no conflicts of interest.

Appendix A. Supplementary data

Supplementary data to this article can be found online at https://doi.org/10.1016/j.jpha.2019.09.006.

References

[1] W. Schneider, K. Schroeter, Aceto-papaverin und Coralyn (Hexadehydro-coralydin), Berichte Der Dtsch. Chem. Gesellschaft (A B Ser. 53 (1920) 1459–1469, https://doi.org/10.1002/cber.19200530824.
[2] S.D. Phillips, R.N. Castle, A review of the chemistry of the antitumor benzo [c] phenanthridine alkaloids nitidine and fagaronine and of the related antitumor alkaloid coralyne, J. Heterocycl. Chem. 18 (1981) 223–232.
[3] K.Y. Zee-Cheng, C.C. Cheng, Practical preparation of coralyne chloride, J. Pharm. Sci. 61 (1972) 969–971.
[4] K.-Y. Zee-Cheng, C.C. Cheng, Common receptor-complement feature among some antileukemic compounds, J. Pharm. Sci. 59 (1970) 1630–1634, https://doi.org/10.1002/jps.2600591118.
[5] K.-Y. Zee-Cheng, K.D. Paull, C.C. Cheng, Experimental antileukemic agents. Coralyne, analogs, and related compounds, J. Med. Chem. 17 (1974) 347–351, https://doi.org/10.1021/jm00249a020.
[6] B. Gatto, M.M. Sanders, C. Yu, et al., Identification of topoisomerase I as the cytotoxic target of the protoberberine alkaloid coralyne, Cancer Res. 56 (1996) 2795–2800.
[7] M. Franceschin, L. Rossetti, A. D'Ambrosio, et al., Natural and synthetic G-quadruplex interactive berberine derivatives, Bioorg. Med. Chem. Lett 16 (2006) 1707–1711, https://doi.org/10.1016/j.bmcl.2005.12.001.
[8] B.S. Patro, B. Maity, S. Chattopadhyay, Topoisomerase inhibitor coralyne photosensitizes DNA, leading to elicitation of Chk2-dependent S-phase checkpoint and p53-independent apoptosis in cancer cells, Antioxidants Redox Signal. 12 (2010) 945–960, https://doi.org/10.1089/ars.2009.2508.
[9] J. Ren, J.B. Chaires, Sequence and structural selectivity of nucleic acid binding ligands, Biochemistry 38 (1999) 16067–16075, https://doi.org/10.1007/s00216-011-4669-0.
[10] J.S. Lee, L.J. Latimer, K.J. Hampel, Coralyne binds tightly to both T.A.T- and C.G.C(+)-containing DNA triplexes, Biochemistry 32 (1993) 5591–5597.
[11] R. Sinha, G.S. Kumar, Interaction of isoquinoline alkaloids with an RNA triplex: structural and thermodynamic studies of berberine, palmatine, and coralyne binding to poly(U).poly(A)(*)poly(U), J. Phys. Chem. B 113 (2009) 13410–13420, https://doi.org/10.1021/jp9069515.
[12] M.M. Islam, R. Sinha, G.S. Kumar, RNA binding small molecules: studies on t-RNA binding by cytotoxic plant alkaloids berberine, palmatine and the comparison to ethidium, Biophys. Chem. 125 (2007) 508–520.
[13] F. Xing, G. Song, J. Ren, et al., Molecular recognition of nucleic acids: coralyne binds strongly to poly(A), FEBS Lett. 579 (2005) 5035–5039, https://doi.org/10.1016/j.febslet.2005.07.091.
[14] K. Bhadra, G.S. Kumar, Interaction of berberine, palmatine, coralyne, and sanguinarine to quadruplex DNA: a comparative spectroscopic and calorimetric study, Biochim. Biophys. Acta Gen. Subj. 1810 (2011) 485–496, https://doi.org/10.1016/j.bbagen.2011.01.011.
[15] A.A. Moraru-Allen, S. Cassidy, J.L.A. Alvarez, et al., Coralyne has a preference for intercalation between TA.T triples in intramolecular DNA triple helices, Nucleic Acids Res. 25 (1997) 1890–1896, https://doi.org/10.1093/nar/25.10.1890.
[16] B. García, S. Ibeas, R. Ruiz, et al., Solvent effects on the thermodynamics and kinetics of coralyne self-aggregation, J. Phys. Chem. B 113 (2009) 188–196, https://doi.org/10.1021/jp807894a.
[17] S. Hazra, M. Hossain, G.S. Kumar, Studies on α-, β-, and γ-cyclodextrin inclusion complexes of isoquinoline alkaloids berberine, palmatine and coralyne, J. Incl. Phenom. Macrocycl. Chem. 78 (2014) 311–323, https://doi.org/10.1007/s10847-013-0301-6.
[18] A.N. Gough, R.L. Jones, W.D. Wilson, Dimerization of coralyne and its propyl analogue and their association with DNA, J. Med. Chem. 22 (1979) 1551–1554.
[19] M. Megyesi, L. Biczók, H. Görner, Dimer-promoted fluorescence quenching of coralyne by binding to anionic polysaccharides, Photochem. Photobiol. Sci. 8 (2009) 556–561, https://doi.org/10.1039/b822649k.
[20] S. Pal, G.S. Kumar, D. Debnath, et al., Interaction of the antitumour alkaloid coralyne with duplex deoxyribonucleic acid structures: spectroscopic and viscometric studies, Indian J. Biochem. Biophys. 35 (1998) 321–332.
[21] K. Padmapriya, R. Barthwal, NMR based structural studies decipher stacking of the alkaloid coralyne to terminal guanines at two different sites in parallel G-quadruplex DNA, [d(TTGGGGT)]4 and [d(TTAGGGT)]4, Biochim. Biophys. Acta Gen. Subj. 1861 (2017) 37–48. https://doi.org/10.1016/j.bbagen.2016.11.011.
[22] A.N. Tripathi, L. Chauhan, P.P. Thankachan, et al., Quantum chemical and nuclear magnetic resonance spectral studies on molecular properties and electronic structure of berberine and berberrubine, Magn. Reson. Chem. 45 (2007) 647–655, https://doi.org/10.1002/mrc.2019.
[23] A.N. Tripathi, K. Bisht, P.P. Thankachan, et al., Quantum chemical and nuclear magnetic resonance spectral studies on molecular properties and electronic structure of palmatine molecule, J. Mol. Struct. 878 (2008) 139–148, https://doi.org/10.1016/j.molstruc.2007.07.046.
[24] A.D. Becke, Density-functional thermochemistry. III. The role of exact exchange, J. Chem. Phys. 98 (1993) 5648–5652.
[25] C. Lee, W. Yang, R.G. Parr, Development of the Colle-Salvetti correlation-energy formula into a functional of the electron density, Phys. Rev. B. 37 (1988) 785–789.
[26] T. Goddard, D. Kneller, Sparky 3-NMR Assignment and Integration Software, University of California, 2006.
[27] I.S. Joung, Ö. Persil Çetinkol, N.V. Hud, et al., Molecular dynamics simulations and coupled nucleotide substitution experiments indicate the nature of A·A base pairing and a putative structure of the coralyne-induced homo-adenine duplex, Nucleic Acids Res. 37 (2009) 7715–7727, https://doi.org/10.1093/nar/gkp730.
[28] J.B. Chaires, N. Dattagupta, D.M. Crothers, Selfassociation of daunomycin, Biochemistry 21 (1982) 3927–3932.
[29] P. Agrawal, S.K. Barthwal, R. Barthwal, Studies on self-aggregation of anthracycline drugs by restrained molecular dynamics approach using nuclear magnetic resonance spectroscopy supported by absorption, fluorescence, diffusion ordered spectroscopy and mass spectrometry, Eur. J. Med. Chem. 44 (2009) 1437–1451, https://doi.org/10.1016/j.ejmech.2008.09.037.
[30] D.B. Davies, D.A. Veselkov, M.P. Evstigneev, et al., Self-association of the antitumour agent novatrone (mitoxantrone) and its hetero-association with caffeine, J. Chem. Soc. Perkin Trans. 2 (2001) 61–67.
[31] C. Shao, M. Grüne, M. Stolte, et al., Perylene bisimide dimer aggregates: fundamental insights into self-assembly by NMR and UV/vis spectroscopy, Chem. Eur J. 18 (2012) 13665–13677, https://doi.org/10.1002/chem.201201661.
[32] L. Gallois, M. Fiallo, A. Garnier-suillerot, Comparison of the interaction of doxorubicin , daunorubicin , idarubicin and idarubicinol with large unilamellar vesicles Circular dichroism study, Biochim. Biophys. Acta (BBA)-Biomembr. 1370 (1998) 31–40.
[33] J. Kapuscinski, Z. Darzynkiewicz, Interactions of antitumor agents ametantrone and mitoxantrone (novatrone) with double-stranded DNA, Biochem. Pharmacol. 34 (1985) 4203–4213.
[34] D.M. Crothers, S.L. Sabol, D.I. Ratner, et al., The behavior of actinomycin in solution, Biochemistry 7 (1968) 1817–1823, https://doi.org/10.1021/bi00845a028.
[35] D.B. Davies, L.N. Djimant, A.N. Veselkov, 1H NMR investigation of self-association of aromatic drug molecules in aqueous solution. Structural and thermodynamical analysis, J. Chem. Soc. Faraday. Trans. 92 (1996) 383–390, https://doi.org/10.1039/FT9969200383.
[36] H.J. Li, D.M. Crothers, Studies of the optical properties of the proflavine–DNA complex, Biopolymers 8 (1969) 217–235, https://doi.org/10.1002/bip.1969.360080208.
[37] C. Giessner-Prettre, B. Pullman, P.N. Borer, et al., Ring-current effects in the nmr of nucleic acids: a graphical approach, Biopolymers 15 (1976) 2277–2286, https://doi.org/10.1002/bip.1976.360151114.
[38] W.J. Harrison, D.L. Mateer, G.J.T. Tiddy, Liquid-crystalline J-aggregates formed by aqueous ionic cyanine dyes, J. Phys. Chem. 100 (1996) 2310–2321, https://doi.org/10.1021/jp952532l.